MICROCHANNEL DEVICES

R. D. Wilson and D. E. Alman
U.S. Department of Energy
Albany Research Center
Albany, OR 97321-2198

ABSTRACT

The fabrication of stainless steel microchannel heat exchangers was examined through microlamination, the process of diffusion bonding precision machined metallic foils. The influence of diffusion bonding parameters, as well as the device geometry on the strength of the bond between the foils and embedded channel integrity was investigated. During diffusion bonding, high temperatures and/or pressures result in well bonded foils, but these conditions cause the embedded channels to deform, which will degrade the efficiency of fluid flow through the channels. Alternatively, low temperatures and/or pressures result in undeformed channels but weakly bonded foils; this causes failure of the device due to fluid leakage. Thus, a processing envelope exists for producing a sound device with no fluid leakage and no degradation of fluid flow properties. The theoretical limit on aspect ratio within two-fluid counter-flow microchannel heat exchangers was also investigated. A counter-flow device is comprised of alternating layers of microchannels, which allow the two fluids to flow in opposite directions separated by fins. A theoretical model for interpreting the span of the fin as a function of the fin thickness was established. The model was verified experimentally by fabricating specimens to simulate the counter-flow device. The results of these investigations were used to aid in the design and processing of prototype microchannel devices.

INTRODUCTION

In recent years, there has been a growing emphasis in manufacturing research on the fabrication of Microtechnology-based Energy and Chemical Systems (MECS). MECS are mesoscopic devices, which use embedded microstructures to enhance heat and mass transfer.[1] By mesoscopic it is meant the size range between micro-scale systems such as microelectronic circuits and microelectromechanical systems (MEMS) and more conventional macro-scale systems such as automobile engines and vacuum pumps. Small characteristic sizes in energy and chemical systems provide the benefits of high rates of heat and mass transfer, large surface-to-volume ratios, and the opportunity of operating at elevated pressures.

One advantage of these MECS or microchannel devices over more conventional devices is that they have more surface area available for heat and mass transfer. This large surface area to volume ratio results in an increase in the overall heat and mass transfer of the device.[2–4] Friedrich and Kang[5] used the term surface area density to quantify this attribute of microchannel devices where surface area density is defined as the ratio of surface area to volume. High aspect ratio (AR) microchannels can have very high surface area densities in excess of 5,000 m^2/m^3 where AR is defined as the ratio of channel width to channel height. Further, devices with high AR microchannels tend to have a low pressure drop when compared with other high surface area density structures (e.g. sponges) thus enhancing the efficiency of the device.

A convenient method of fabricating microchannel devices is through a process termed microlamination. Microlamination is the patterning and bonding of thin layers of material, called laminae, into a monolithic device.[1,6–14] Microlamination involves three steps: (1) lamina (or foil) patterning, (2) laminae registration (alignment), and (3) laminae bonding to produce a monolithic device. Figure 1 shows the microlamination of a general-purpose microchannel array. In all, microchannel arrays have been constructed in a wide

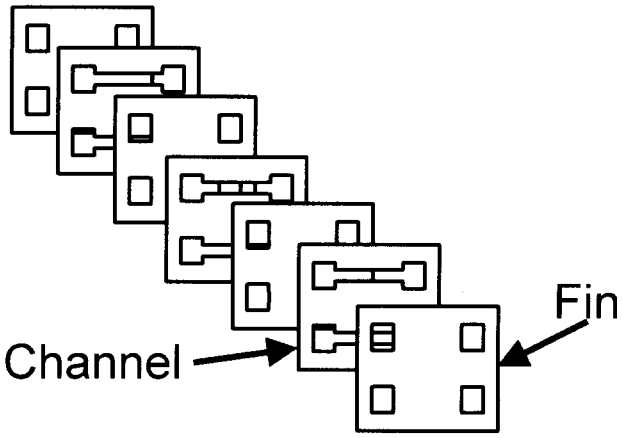

Fig. 1. Schematic of a dual microchannel array.

array of materials including copper, stainless steel, intermetallics and various polymers with features as small as tens of micrometers.[6–14]

In the case of heat transfer, a typical micro-scale heat exchanger involves the transmission of heat from one fluid stream into a second fluid stream. Several different device architectures can be used to accomplish this task. The most efficient heat transfer methods tend to interleave the two fluids with alternating fluids in the succession of channels. To further increase the efficiency of the device, cross-flow and counter-flow architectures can be used to provide better temperature distribution along the length of the heat exchanger when compared to co-flow heat exchangers.[15] Whereas, in the case of single fluid flow, microchannels with relatively high ARs have been fabricated successfully,[16] the aspect ratio is constrained in two-fluid micro-scale heat exchangers because of the complex geometry.

This research investigates the fabrication of microchannel devices via microlamination. The influence of diffusion processing parameters on the integrity of the microchannels and the influence of the architecture of cross-flow devices were investigated.

INFLUENCE OF DIFFUSION BONDING PARAMETERS

Diffusion bonding is commonly used to join metallic and ceramic structures. Commonly, in this process, solid components are heated to temperature and pressure, and held at these conditions for a period of time necessary for diffusion to occur and join the components. For conventional joining, the diffusion bonding parameters are optimized based on the strength of the bond between the components. However, the internal embedded features complicate diffusion bonding of microchannel devices. During processing the foils must be sufficiently bonded together to prevent fluid leakage, but these must not compromise the dimension of the embedded feature (e.g., cause the channels to warp or collapse). Therefore, it is important to understand not only how the bonding parameters affect the strength of the bond between the foils, but also understand how the parameters affect the design features of the device.

A two level–four factorial experiment was designed to evaluate the influence of processing temperature, time, pressure and the foil surface condition on the bond strength and channel integrity of diffusion bonded stainless steel foils. Stainless steel sheets were precision machined such that each diffusion bonded coupon would include a channel for pressure drop measurements and a double lap-joint tensile specimen for bond strength measurements (Fig. 2). The processing conditions were varied as follows: time 2 and 10 hours, temperature 600 and 900°C, nominal applied force 36 and 3600 lb. Prior to bonding the surface of the foils was cleaned by either simply degreasing (in a 50/50 alcohol/acetone mixture and ultrasonically cleaned for 15 minutes) or polishing and etching (hand polishing the foils against 600 grit

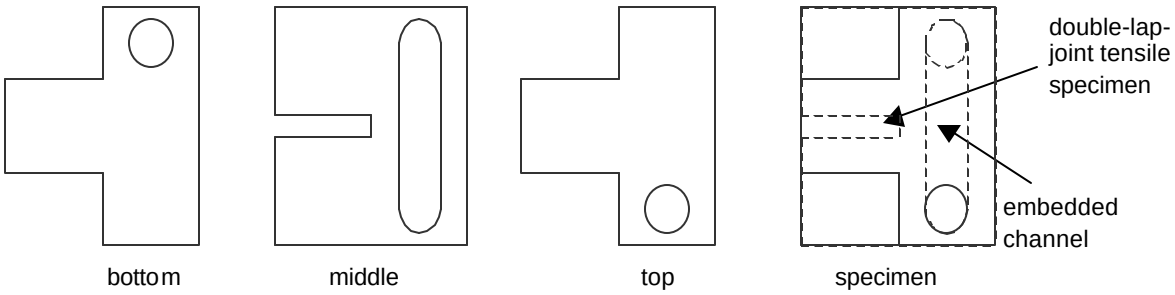

Fig. 2. Schematic of double-lap-joint tensile and pressure drop specimen for diffusion bonding experiments.

abrasive paper; followed, by immersing the foils in a 50/50 alcohol/acetone mixture and ultrasonically cleaning for 15 minutes; and finally, by etching the foils in a 10 percent (by volume) HCl solution for 15 minutes). All experiments were completed with triplicate specimens for each condition produced. Pressure drop samples were sent to Oregon State University (OSU) for testing. The double-lap joint bond strength tensile specimens were tensile tested at ARC.

The results of the initial study revealed that processing temperature and pressure significantly influenced both the strength of the bond between foil layers and flow of the fluid through the channel. Surface condition and process time did not significantly influence these properties. In order to examine the effect of temperature and pressure further, an experiment was performed using the parameters shown in Table 1.

Table 1 also lists the bond strengths for each processing condition. Clearly, the higher temperature and pressure resulted in stronger bonded foils with less variance. However, as shown in Fig. 3a, high temperatures and pressures caused the embedded channel to deform. Excessive warpage of the structure will cause the channels to completely collapse which will prevent fluid flow through the channels. The higher temperature coupled with the lower pressure proved optimal for producing a sound device (Fig. 3b). That is, a device with well bonded foils and the dimensions of the internal feature not compromised. These experiments were used to identify the bonding parameters for producing several prototype stainless steel microchannel heat-exchangers.

Table 1. Influence of diffusion bonding parameters on bond strength of double-lap-joint tensile specimen

Diffusion bonding conditions			Max stress (MPa)	Yield stress (MPa)	Fracture location
Temperature (°C)	Time (h)	Nominal pressure (MPa)			
750	2	6.2	201±107	93 ± 24	In bond
750	2	1.4	11	9	In bond
900	2	6.2	>364 ± 32	93 ± 14	Outside bond
900	2	1.4	216 ± 83	86 ± 16	In bond

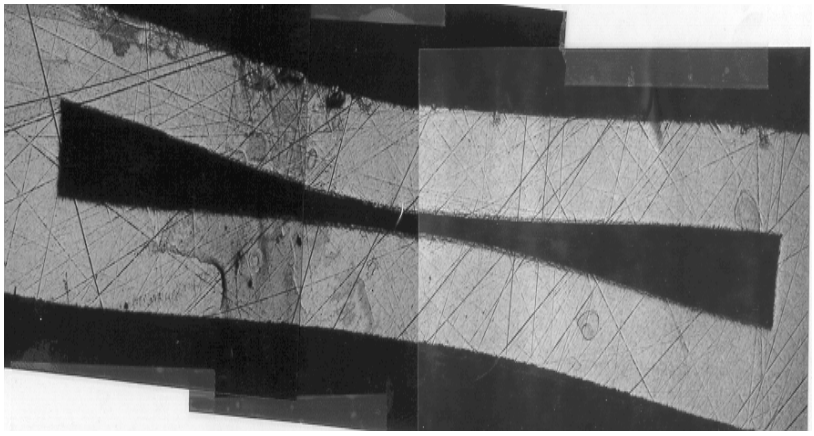

(a)

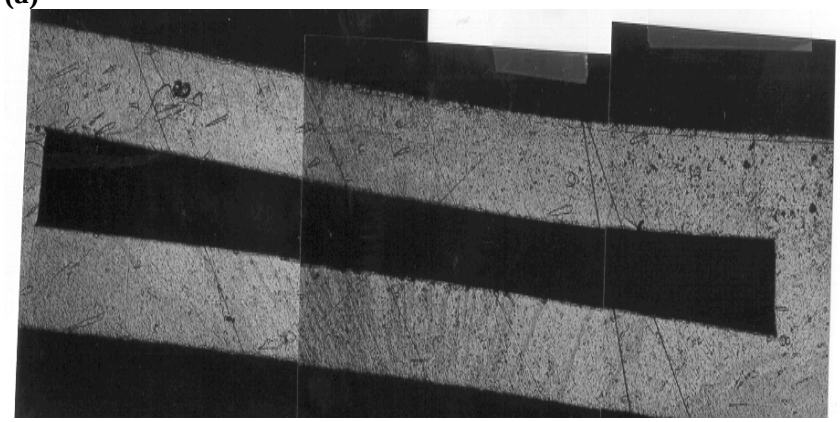

(b)

Fig. 3. Cross section of embedded channel for pressure drop measurements for the diffusion bonding experiments: (a) 900°C-6.2MPa-2h; (n) 900°C–1.2 MPa-2h.

LIMITS ON THE ASPECT RATIO FOR CROSS-FLOW MICROCHANNEL DEVICES

The cross-flow device is comprised of alternating layers of microchannels, which allow multiple fluids to flow in opposite (or different) directions in individual channels separated by fins. The architecture of these devices inevitably must consist of a region where the channels (hence fluids) must cross each other. This causes difficulties during diffusion bonding. During diffusion bonding a pressure is applied to the top and bottom surfaces of the stack of foils at an elevated temperature. Pressure is directly transmitted uniformly through the device except at regions where the microchannels cross each other (the neck of each microchannel). Where this “gap” exists between the individual foils, pressure is not transmitted directly between adjacent sheets during diffusion bonding. This lack of directly transmitted pressure may cause the foils to remain unbonded during processing, as shown in Fig. 4a. In this case leakage will occur in the device and the two fluids will mix. Figure 4b shows a region where pressure was directly transmitted through all of the adjacent sheets. Excellent bonding occurred in this region, and the two fluids remain separated by fins. This “gap” problem is inherent to all cross-flow micro-channel devices that contain two or more fluids produced via any bonding method (e.g., diffusion bonding, diffusion soldering, reactive bonding, etc).

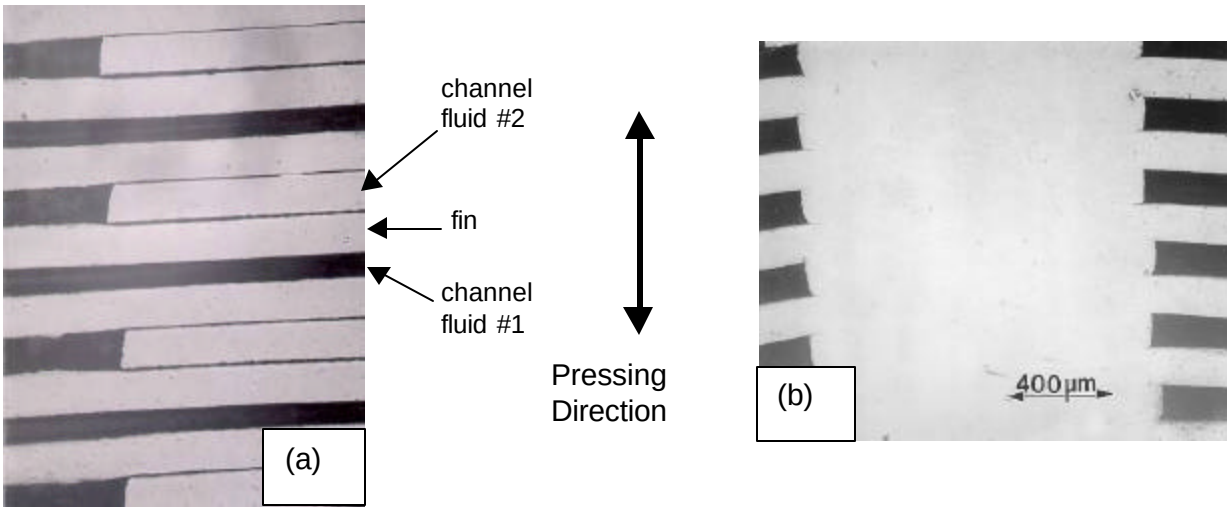

Fig. 4. Cross section of a counter-flow microchannel device: (a) showing a section where through which bonding pressure was not transmitted; and (b) region where pressure was transmitted. In (a) the fin above the channel did not bond causing leakage of the fluids.

In experience, the width of the channel has to be constrained to a dimension where bonding will occur. The limit on the width of the channel at which bonding takes place depends on the thickness of the foil. In other words, as the thickness of the fins above and below the neck of the microchannels increases, the neck can be made wider. Assuming that the thickness of all the fins remains constant, the ratio of the channel span in the neck region to the lamina thickness is the aspect ratio. Therefore, there will be some optimum aspect ratio at which all foils will bond.

Paul et. al.,[17] recognized that the cause of the leakage problem is the deflection of a fin during bonding,and to model this phenomenon, a free-body diagram of an unsupported fin was developed (Fig. 5). The major factor, which contributes to the deflection of the fin, is a pressure gradient (w) created at the ends of the fin due to compression of the adjacent foils under the bonding pressure. This gradient results in a downward bending moment on the fin. To simplify the deflection model, only the deflection due to compression of the adjacent foil stack under load was considered.

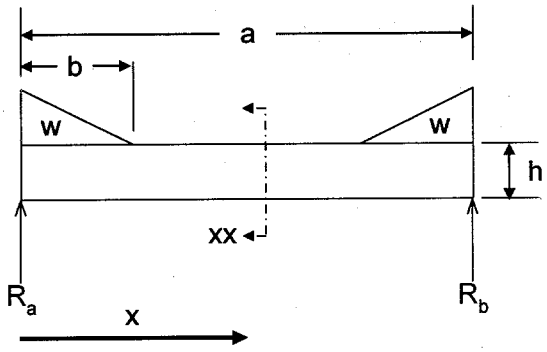

Fig. 5. Distribution of force on the portion of fin above the lower channel.

The span of the fin is assumed to be a distance (a) and its thickness is (h). The effect of the bonding pressure (P) on the fin is to compress the ends of the fin only with the pressure decreasing into the channel. If this pressure gradient (w) is assumed to be a triangular load acting over a distance of (b) on the fin, the resulting forces R_a and R_b can be reduced to:

$$R_a = R_b = \frac{bw}{2} \tag{1}$$

Taking moments about a cross-section XX gives:

$$M_{XX} = R_a x - \frac{1}{2} bw\left(x - \frac{1}{3} b\right) = \frac{1}{2} bwx - \frac{1}{2} bwx + \frac{1}{6} b^2 w = \frac{1}{6} b^2 w \tag{2}$$

The equation for moment is given by:

$$EI \frac{d^2 y}{dx^2} = M_{XX} = \frac{1}{6} b^2 w \tag{3}$$

Solving by the double integration method and applying the boundary conditions as follows:

i) $x = 0, y = 0$, and

ii) $x = \frac{a}{2}, \frac{dy}{dx} = 0$

yields:

$$EIy = \frac{1}{12} b^2 wx(x - a) \tag{4}$$

The maximum elastic in-process deflection, y_{comp}, is obtained at the center of the beam. Therefore, substituting $x=a/2$ in Equation 4 gives:

$$y_{comp} = -\frac{1}{48 EI} a^2 b^2 w \tag{5}$$

It was assumed that for bonding to occur, the load *w* should be applied through out the width of the beam. Therefore, b = a where both a and b represent the width of the channel. Further, assuming that w = Pd where P is the original bonding pressure and d is the unconstrained depth of the fin into the paper, the area moment of inertia, I, is given by:

$$I = \frac{dh^3}{12} \tag{6}$$

Therefore, Equation 5 can be rewritten as:

$$y_{comp} = -\frac{1}{48E\left(\frac{dh^3}{12}\right)}(a^4 Pd) = -\frac{P}{4E}\left[\frac{a^4}{h^3}\right] \tag{7}$$

Equation 7 gives us an estimate of deflection in the fin just below the channel. It can be rewritten as:

$$a^4 = h^3\left[\frac{-4Ey_{comp}}{P}\right] \tag{8}$$

For a given set of bonding conditions (e.g., temperature, pressure), the quantity $\frac{-4Ey_{comp}}{P}$ is constant. Therefore, Equation 8 can be rewritten as:

$$\frac{a^4}{h^3} = K_b \tag{9}$$

where K_b is a bonding constant that is a function of the bonding conditions and geometry of the device.

Specimens were designed to simulate the necked region of the counter-flow device as shown in Fig. 6. The stacking order of the device was alternating foils of blanks (fins) followed by a slot (channel). Every other slot was flipped to produce the required geometry. Three specimens of 0.508 mm thick 304-SS with a channel span (slots) of 2.54 mm, 3.175 mm, and 5.08 mm and specimens of 0.254 mm thick foils with a channel span of 1.524 mm, 2.54 mm, and 5.08 mm were diffusion bonded. The bonding of unsupported fins was evaluated by metallographic techniques. The results revealed that for the 0.508 mm foils, the specimens with 2.54 mm and 3.175 mm spans were bonded below and above the channel, whereas small gaps between shims were detected for the specimen with the 5.08 mm span. For the 0.254 mm foils, only a span length of 1.524 mm produced good bonding between the foils. The graph in Fig. 7 reveals that there is good agreement between the experimental results and values predicted by the theoretical model. The solid curve is the predicated demarcation between bonding and leakage as a function of the aspect ratio of the device architecture predicated from by model. The symbols correspond to the experimental results for the two shim thickness.

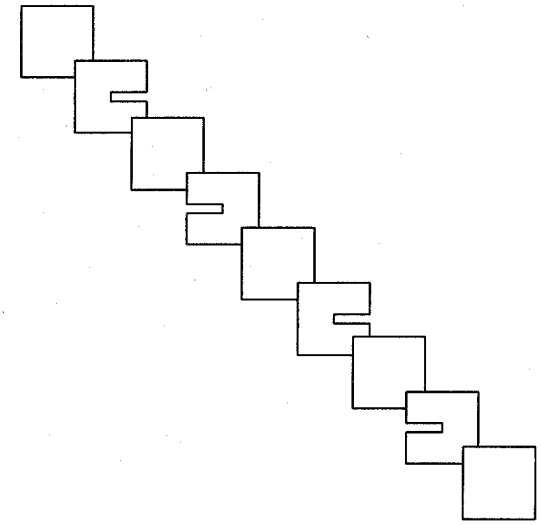

Fig. 6. Schematic of the test specimen used to simulate the necked region of a counter flow device.

The curve shown in Fig. 7 is generated by Equation 9 is only for 304 stainless steel diffusion bonded at 900°C and 5.86 MPa and is not generalizable to all bonding methods and conditions. In addition to the material and geometry constants in the bonding constant K_b, a value for y_{comp} is required. y_{comp} is considered to be the maximum in-process, elastic deflection that will still yield a good bond. It is assumed that the value for y_{comp} would change for a new set of bonding conditions. Also the values of y_{comp} are thought to be liberal as they assume that all of the deflection is due to the compression of the laminae stack. In addition to the pressure gradient, *w*, caused by the compression of the foil stack, an end load could be produced laterally on the fin due to both Poisson's ratio and thermal expansion, which may result in the buckling of the fin.[17] Regardless, the model can be used to aid in the design of 304Ss microchannel devices provided the diffusion bonding parameters conform to the prescribed conditions. Figure 8 shows metallographic cross sections of the neck region of two prototype microchannel heat exchangers diffusion bonded under identical conditions and of similar architectures. Figure 8a shows the device in which the aspect ratio exceeded the limitation predicted the model. Clearly, the foils did not bond and this device failed due to mixture of the fluids. The cross section shown in Fig. 8b, shows a device in which the aspect ratio did not exceed the limitation described by the model. In this case the foils

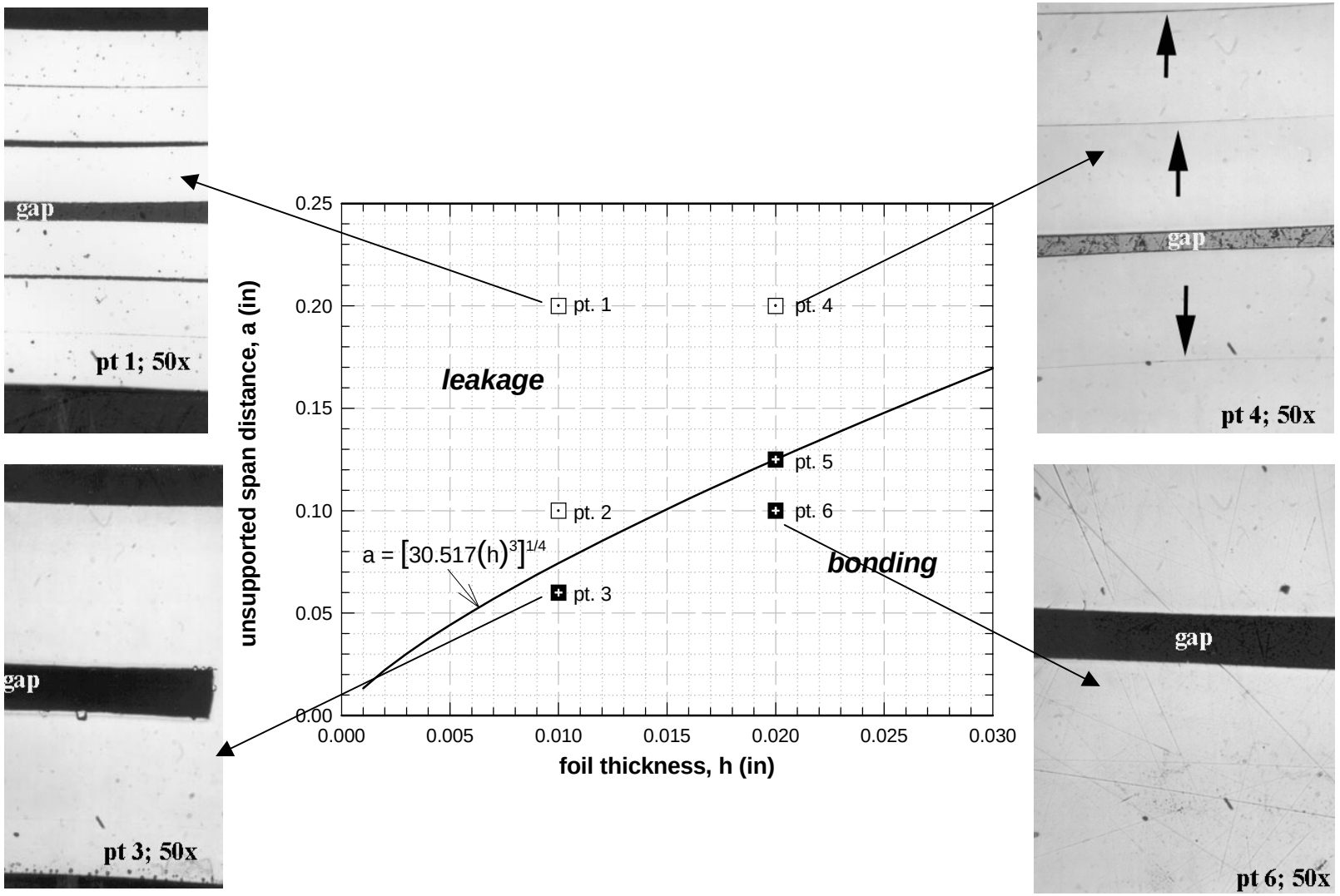

Fig. 7. Comparison between experimental results and theoretical model for unsupported span aspect ratio.

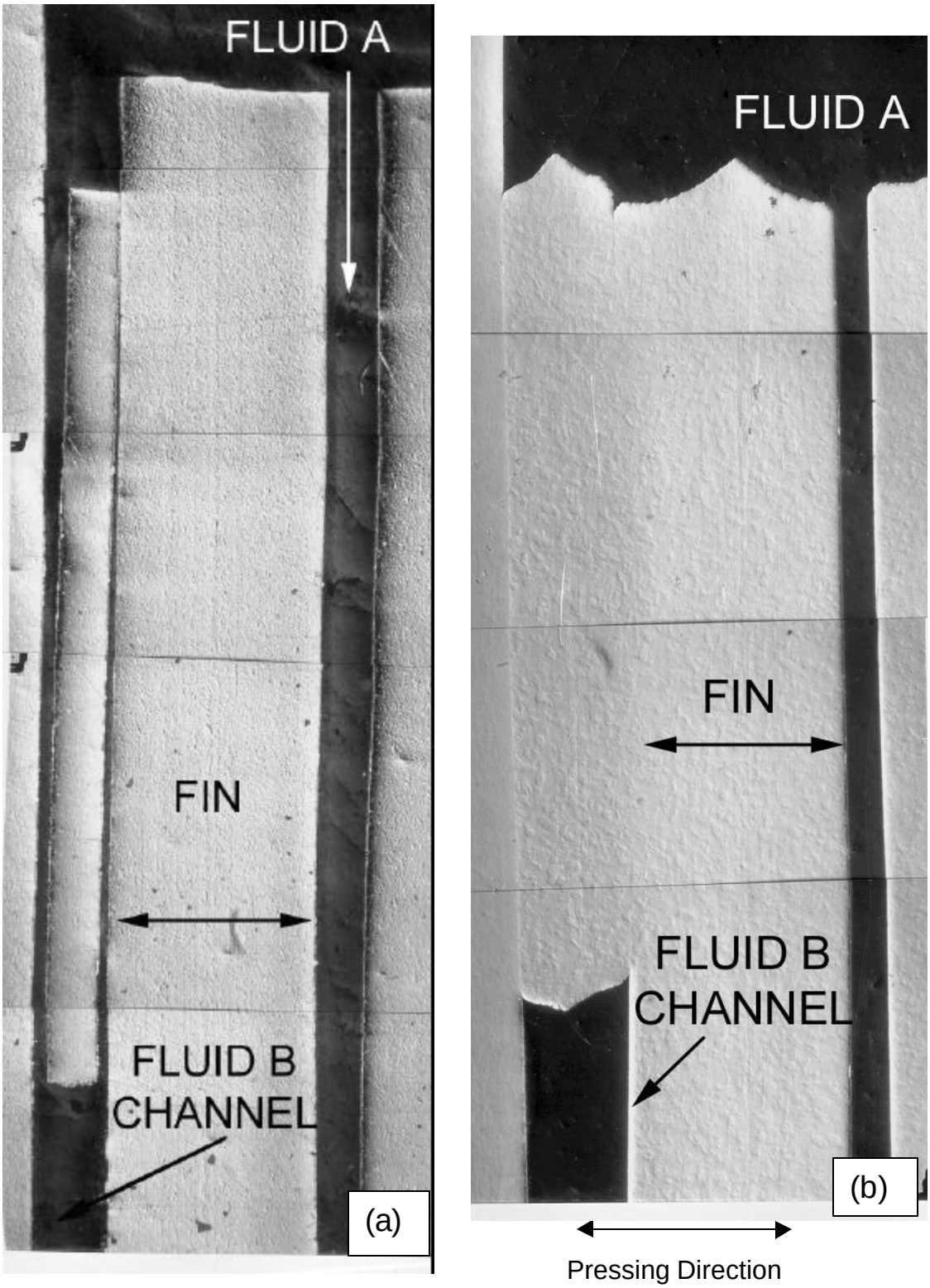

Fig. 8. Cross sections of prototype counter-flow microchannel heat exchangers: (a) aspect ratio of fin exceeded theoretical limit; and (b) aspect ratio of fin did not exceed theoretical limit. In (a) poor bonding between the foils was achieved during processing , while in (b) good bond was achieved between the foils during processing.

bonded producing a sound device. Thus, the model and approach can be an invaluable aid in the design of microchannel devices.

APPLICATIONS

In conjunction with Oregon State University and a CRADA partner, Zess Technologies, Inc, several heat-exchangers with different microchannel arrays were fabricated at the Albany Research Center. Figure 8b shows a sound prototype counter-flow microchannel heat-exchanger produced via microlamination of 304 stainless steel foils. Several diverse applications for these devices under consideration include: compact heat-exchangers for thermal management of electronic devices, compact heat-exchangers for transportation applications, and for recuperators to increase the efficiency of small 40 kw turbines used for power generation.

For the latter application, it is estimated that a properly designed microchannel heat exchanger would be four (4) times smaller than a standard heat-exchanger.[18] This may imply that microchannel technology might enable the production of recuperators for advanced microturbine materials from a more expensive and more creep resistant material than standard alloys. That is, if the physical design of the microchannel heat-exchanger is smaller than a conventional design, the microchannel design will require less material, and thus, may enable a more expensive alloy to be cost effective for this application.

Currently, Idaho National Engineering Laboratory, Oregon State University and the Albany Research Center are collaborating on producing a microchannel chemical reactor to catalytically destroy volatile, toxic organic chemicals. This project is designed to demonstrate the efficiency of micro-reactors to process the gases derived from heating drums of TRU (Pu238) wastes contaminated with volatile organics prior to the shipment of the containers to a disposal location. Steam reforming offers the potential for rapid and efficient destruction of volatile chlorinated organic matter by reforming hydrocarbons to a mixture of hydrogen and oxides of carbon that can then be oxidized separately in a catalytic oxidation unit. This accomplishes the required destruction while minimizing the potential for products of incomplete combustion. For this particular application the channels of the reactors are coated with a catalyst material. Thus the material selected for producing the device must not only be highly corrosive resistant, but also must not react with the catalyst. Currently, the suitability of using aluminide alloys (e.g., FeAl or NiAl) for this application is being evaluated. Also, the utilization of a reactive foil lamination technique[19, 20] for the production of such heat exchanges is being investigated.[12,21]

SUMMARY

The processing of microchannel devices by microlamination of precision machined 304 stainless steel was investigated. The internal features of the device complicate the diffusion bonding process. These features must not be altered as a result processing. An investigation on limits of aspect ratio for counter-flow heat exchangers was performed The results reveal that for a given set of bonding conditions there exists a maximum permissible value of elastic fin deflection during bonding beyond which leakage is bound to occur. A model was developed to predict this aspect ratio. This model was used to produce a prototype micochannel device.

ACKNOWLEDGEMENT

The authors are extremely grateful to Professor B. K. Paul of the Industrial and Manufacturing Engineering Department, Oregon State University, Corvallis, OR, 97331, for his active collaboration in this research**.**

REFERENCES

1. B. K. Paul, and R. B. Peterson, "Microlamination for Microtechnology-based Energy, Chemical, and Biological Systems," *ASME IMECE,* Nashville, Tennessee, November 15–20, 1999, pp. 45–52.
2. K. P. Brooks, P. M. Martin, M. K. Drost, and C. J. Call, "Mesoscale Combustor/Evaporator Development," *ASME IMECE Conference, Nashville, TN*, November 1999, pp. 37–43.
3. J. H. Wang, H. Y. Yeh, and R. J. Shyu, "Thermal-Hydraulic Characteristic of Microheat Exchangers," *American Society of Mechanical Engineers, Dynamic Systems and Control Division* (Publication) (DSC v32 Dec 1–6 1991), pp. 331–339.
4. X. F. Peng, B. X. Wang, G. P. Peterson, and H. B. Ma, "Experimental Investigation of Heat Transfer in Flat Plates with Rectangular Microchannels," *International Journal of Heat and Mass Transfer* (v38, n1, 1995), pp. 127–137.
5. C. R. Friedrich and S. D. Kang, "Microheat Exchangers Fabricated by Diamond Machining," *Precision Engineering* (v16, n1, January 1994), pp. 56–59.
6. R. S. Wegeng, C. J. Call, and M. K. Drost, "Chemical Systems Miniaturization," *1996 AIChE Spring Meeting,* New Orleans, 1996.
7. P. M. Martin, W. D. Bennett, and J. W. Johnson, "Microchannel Heat Exchangers for Advanced Climate Control," *Proc. SPIE* (v2639, 1996), pp. 82–88.
8. D. W. Matson, P. M. Martin, W. D. Bennett, D. C. Stewart, and J. W. Johnson, "Laser Micromachined Microchannel Solvent Separator," *Proc. SPIE,* (v3223, 1997), pp. 253–259.
9. G. Jovanovic, J. Zaworski, T. Plant, and B. Paul, *Proc. 3rd Intl. Conf. on Microreaction Technology* (Frankfurt, Germany), 1999, in press.
10. D. W. Matson, P. M. Martin, A. Y. Tonkovich, and G. L. Roberts, "Fabrication of a Stainless Steel Microchannel Microcombustor Using a Lamination Process," *Proc. SPIE* (v3514, 1998), pp. 386–392.
11. Y. Tonkovich, J. L. Zilka, Y. Wang, M. J. LaMont, S. Fitzgerald, D. P. Vanderwiel, and R. S. Wegeng, "Microchannel Chemical Reactors for Fuel Processing Applications. II. Compact Fuel Vaporization," *Proc. 3rd Intl. Conf. on Microreaction Technology* (Frankfurt, Germany), 1999, in press.
12. B, K. Paul, T. Dewey, D. Alman, and R. D. Wilson, "Intermetallic Microlamination for High-Temperature Reactors," *4th Int. Conf. Microreaction Tech.*, Atlanta, GA, March 5–9, 2000, pp. 236–243.
13. B. K. Paul, and T. Terhaar, "Comparison of two passive microvalve designs for microlamination architectures," *J Micromech. Microengr.*, (v10, 2000), pp. 15–20.
14. P. M. Martin, D. W. Matson, W. D. Bennett, and D. J. Hammerstrom, "Fabrication of plastic microfluidic components," *Proc. SPIE* (v3515, 1998), pp. 172–176.
15. S. Kakac and H. Liu, *Heat Exchangers-Selection, Rating, and Thermal Design*, CRC Press, Boca Raton, 1997.
16. B. K. Paul, R. B. Peterson, and W. Wattanutchariya, "The Effect of Shape Variation on the Performance of High-Aspect-Ratio, Metal Microchannel Arrays," *IMRET 3: Proceedings of the Third International Conference on Microreaction Technology, Springer-New York,* 1999, pp. 53–61.
17. B. K. Paul, H. Hasan, J, S. Thomas, R. D. Wilson, and D. E. Alman, "Limits on Aspect Ratio in Two-Fluid Micro-Sacle Heat Exchangers," to be presented at NAMRC-XXIX, May 22–25, 2001, Gainseville, FL and published in Trans. NAMRI/SME, vol. XXIX, SME, Dearborn, MI, 2001.

18. Private Communication, Jim Zess, Zess Technologies, Inc, Jan 2000.
19. J. C. Rawers, D. E. Alman, and A. V. Petty, Jr., U.S. Patent No. 5,564,620.
20. D. E. Alman, C. P. Dogan, J. A. Hawk, and J. C. Rawers, Mater. Sci. Engr. A192/193, 1995, p. 624.
21. D. E. Alman, R. D. Wilson, and B.K. Paul, “NiAl MECS Devices” to be presented at NAMRC-XXIX, May 22–25, 2001, Gainseville, Fl. and published in Trans. NAMRI/SME, vol. XXIX, SME, Dearborn, MI, 2001.